



ISSN: 0067-2904  
GIF: 0.851

## Synthesis of gold nanoparticles using ceftriaxone sodium as a reducing and stabilizing agent

Ahlam Jameel Abdulghani \*, Saja Khalil Mohuee

University of Baghdad, Department of Chemistry, College of Science, Baghdad, Iraq

### Abstract

The synthesis of gold nanoparticles AuNPs was achieved by the reduction of sodium tetrachloroaurate (III) ( $\text{NaAuCl}_4$ ) with ceftriaxone sodium (CR) in aqueous solutions without the use of other reducing agent. The effect of reactants concentration, temperature and pH on the sizes and morphology of AuNPs were also studied. The synthesized AuNPs were characterized by UV- visible spectroscopy, X-ray diffraction (XRD), scanning electron microscope (SEM), and atomic force microscope (AFM) analysis. Conjugation of antibiotic with the nanoparticles was characterized by FTIR spectrophotometry.

**Keywords:** Ceftriaxone, AuNPs, surface plasmon resonance, antibacterial activity.

### تحضير دقائق الذهب النانوية باستخدام سفتراياكسون الصوديوم كعامل مختزل وعامل استقرار

احلام جميل عبد الغني \*, سجي خليل محي

جامعة بغداد، كلية العلوم، قسم الكيمياء، بغداد، العراق

### الخلاصة

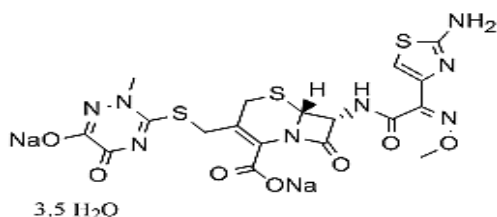
تم تحقيق تحضير دقائق الذهب النانوية باختزال رباعي كلوراوراتاالصوديوم (III) ( $\text{NaAuCl}_4$ ) بواسطة سفتراياكسون الصوديوم (CR) في المحاليل المائية بدون استخدام عامل مختزل اخر. كما تمت دراسة تأثير تركيز المتفاعلات ودرجات الحرارة والذالة الحامضية على حجوم واشكال دقائق الذهب النانوية. شخصت دقائق الذهب النانوية المحضرة بواسطة تحاليل مطيافية الاشعة فوق البنفسجية - المرئية وحيود الاشعة السينية (XRD) والمجهر الالكتروني الماسح (SEM) ومجهر القوة الذرية (AFM). تم تشخيص ارتباط المضاد الحيوي مع الدقائق النانوية بواسطة مطيافية الاشعة تحت الحمراء (FTIR).

### Introduction

A wide range of  $\beta$ -lactam antibiotics have been used as capping agents, reducing agent or both in the synthesis of different shapes and sizes of antibiotic conjugated AuNPs like cefaclor[1], amoxicillin[2], ampicillin[3], streptomycin, kanamycin[4], cefazolin[5], cefotaxim[6], cefuraxime and cefixime[7], at different conditions of pH, temperature and reactant concentrations. Some of these conjugates showed enhanced antibacterial and antimicrobial activities compared with the parent drug [1-4]. Ceftriaxone sodium (Z)-7-[2-(2-aminothiazol-4-yl)-2-methoxyiminoacetylamido]-3-[2,5-dihydro-6-hydroxy-2-methyl-5-oxo-1,2,4-triazin-3-yl] thio methyl]-3-cephem-4-carboxylic acid disodium salt sesquaterhydrate is a third-generation semi-synthetic bactericidal cephalosporin  $\beta$ -lactam antibiotic that has been used in the treatment of bacterial infections caused by pathogenic gram-negative and a wide range of gram-positive bacteria[8-17]. The presence of many binding sites such as the free amino group,  $\beta$ -lactam carbonyl and amide nitrogens makes the drug molecule

\*Email:ahlamjameel@scbaghdad.edu.iq

capable of forming different metal chelates, as well as good polar binding sites for conjugation with AuNPs which may change the toxicological and biological performance of the drug [13,18]. Few articles have been published on using ceftriaxone as capping and stabilizing agent in the synthesis of AuNPs in the presence of reducing agent such as sodium borohydride [7,14,19].



### Chemical structure of ceftriaxone (CR)

It has been reported by M. Aslam et al, that gold nanoparticles can be prepared in water directly by complexation of Au (III) ions with alkylamine, aromatic and poly amine molecules where they act as reducing agents and then subsequently covalently stabilize the gold particles [15] which may affect the rate of growth and nucleation of synthesized nanoparticles [16]. As a primary amine group carrier, now work has been published on using CR as a reducing agent to prepare gold nanoparticles. In this work we investigated the synthesis of AuNPs by CR as reducing and capping agent and studied the effect of concentration, temperature and pH on the rate of synthesis spectrophotometrically by studying the change in position and intensity of surface plasmon resonance band at 520- 550nm. The AuNPs were characterized by FT-IR, SEM, AFM and XRD.

## Materials and Methods

### 1. Chemicals

The following chemicals were used as received from suppliers: Ceftriaxone sodium ( $C_{18}H_{16}N_8O_7S_3Na_2 \cdot 3.5H_2O$ ) (LDP), sodium tetrachloroaurate(III) dihydrate ( $NaAuCl_4 \cdot 2H_2O$ ) (BDH), potassium dihydrogen orthophosphate  $KH_2PO_4$ , 99% (Fluka), dipotassium hydrogenorthophosphate,  $K_2HPO_4$ , 99%, (Fluka), phosphoric acid  $H_3PO_4$  Analar (BDH).

### 2. Instruments

Electronic spectra for prepared solutions in the (UV-Visible) region (200-1100 nm) solvents were recorded on SHIMADZU 1800 Double Beam UV-Visible spectrophotometer. The (FTIR) spectra of the studied solutions were obtained using SHIMADZU FT-IR 8400S Fourier transforms, within the wavenumber region between 4000 and 400  $cm^{-1}$  using KBr disc and 4000-200  $cm^{-1}$  by using CsI disc. Separation of nanoparticles by centrifugation rpm for using CENTERFUGE C 41 7800 14000 r.p.m., Jouan, (France) SEM images were acquired using the instruments (Tescan Vega III Czech) and (KYKY-EM3200). AFM images were acquired using AFM model AA 3000 SPM 220 V-Angstrom Advanced INC. USA. Solutions were prepared by applying few drops of metal nanoparticles solutions on a glass slide followed by vacuum drying. XRD measurements were performed using a SHIMADZU XRD-6000 x-ray diffraction spectrometer.

### 3. Preparation of solutions

A stock aqueous solution of the gold salt  $NaAuCl_4 \cdot 2H_2O$ , ( $2.5 \times 10^{-3}$  M), was prepared by dissolving 0.1 g of  $NaAuCl_4 \cdot 2H_2O$  in 100 ml distilled deionized water (DDW) in 100 ml volumetric flask. A standard solution of  $AuCl_4^-$  ( $2.5 \times 10^{-4}$  M) was prepared by diluting 10 ml of the stock solution to 100 ml with (DDW) in a 100 ml volumetric flask. An aqueous solution of the antibiotic ( $1.51 \times 10^{-3}$  M) was prepared by dissolving 0.1g of ceftriaxone sodium in 100 ml deionized water (DDW) in 100 ml volumetric. A standard solution of the antibiotic ( $1.51 \times 10^{-4}$  M) was prepared by diluting 10 ml of the stock solution to 100 ml with (DDW).

### 4. Optimization synthesis of GNPs

#### Effect of metal ion concentration

One ml aliquots of standard solution of ceftriaxone (CR) ( $1.51 \times 10^{-4}$  M) in volumetric flask were added to ten different volumes of  $AuCl_4^-$  standard solutions ( $2.5 \times 10^{-4}$  M) (0.25, 0.5, 0.75, 1.0, 1.25, 1.5, 2.0, 2.5, 3.0, and 3.5 ml) in 5 ml volumetric flasks, followed by dilution to 5 ml with DDW.

The resulting concentration of CR was ( $3.02 \times 10^{-5} \text{M}$ ), while those of  $\text{AuCl}_4^-$  ( $1.25 \times 10^{-5}$ ,  $2.5 \times 10^{-5}$ ,  $3.75 \times 10^{-5}$ ,  $5 \times 10^{-5}$ ,  $6.2 \times 10^{-5}$ ,  $7.5 \times 10^{-5}$ ,  $1 \times 10^{-4}$ ,  $1.25 \times 10^{-4}$ ,  $1.5 \times 10^{-4}$  and  $1.75 \times 10^{-4} \text{M}$  respectively), and the concentration ratio of CR/Au(III) were : (2.416, 1.208, 0.805, 0.604, 0.487, 0.402, 0.302, 0.241, 0.201 and 0.172) respectively. The absorbance of each solution was measured with time at room temperature; choose the optimum CR/Au (III) concentration ratio.

#### Effect of ligand concentration

To 1ml aliquots  $\text{AuCl}_4^-$  ( $2.5 \times 10^{-4} \text{M}$ ) in ten volumetric flasks were added different volumes of CR ( $1.51 \times 10^{-4} \text{M}$ ) (0.25, 0.5, 0.75, 1.0, 1.25, 1.5, 2.0, 2.5, 3.0, and 3.5ml). The volumes were completed to 5ml with DDW. The final concentration of  $\text{AuCl}_4^-$  was ( $5 \times 10^{-5} \text{M}$ ), while the concentrations of CR were : ( $7.6 \times 10^{-6}$ ,  $1.51 \times 10^{-5}$ ,  $2.25 \times 10^{-5}$ ,  $3 \times 10^{-5}$ ,  $3.7 \times 10^{-5}$ ,  $4.5 \times 10^{-5}$ ,  $6.04 \times 10^{-5}$ ,  $7.55 \times 10^{-5}$ ,  $9.06 \times 10^{-5}$  and  $1.05 \times 10^{-4} \text{M}$  respectively), and the concentration ratio of CR/Au(III) in the ten solutions were (0.152, 0.302, 0.45, 0.6, 0.74, 0.9, 1.208, 1.51, 1.812 and 2.1). The absorbance of each solution was measured with time at room temperature after 1h, 24h, 48h, 1week, 2w 3w and 4w, to choose the optimum CR/Au(III) concentration ratio.

#### Effect of Temperature

Ten (5ml) solution containing the selected concentration ratio of CR/Au (III) were heated for 5minutes at (35, 40, 45, 50, 55, 60, 65, 70, 75 and 80 °C respectively), in a water bath. The absorbance of each solution mixture in the UV-visible region was measured with time after being cooled to room temperature.

#### Effect of heating time

Ten (5 ml) solutions containing the selected CR/Au(III) concentration ratio (0.172), were heated at the selected temperature (40 °C) for different heating times (5, 10, 15, 20, 25, 30, 35, 40, 45 and 60 min respectively). The absorbance of each solution mixture in the UV-visible region was measured after being cooled to room temperature.

#### Effect of pH

The synthesis of AuNPs in solutions CR was studied by uv-visible spectrophotometry at different pH values (2.44, 3.38, 4.26, 5.83, 6.33, 7.20, 8.27, 9.03, 10.30, 11.18), of solutions containing the selected CR/Au(III) concentration ratio (0.172), using the appropriate buffer.

## Results and discussion

### 1. UV-Vis spectrophotometry

#### Concentration effect

Figures -1 (A and B) show the uv-visible spectra of CR,  $\text{AuCl}_4^-$  and the mixture of CR with  $\text{AuCl}_4^-$  (1A) and CR,  $\text{AuCl}_4^-$  and AuNPs (1B) prepared from mixing 3.5ml of  $\text{AuCl}_4^-$  ( $2.5 \times 10^{-4} \text{M}$ ) with 1 ml of CR ( $1.51 \times 10^{-4} \text{M}$ ) diluted to 5ml and the final concentration ratio of solution CR/Au(III) in this solution was (0.172). The pH of solution was 4.83.

The spectrum of CR displayed two high intensity bands at  $\lambda$  272 and 239 nm attributed to  $\pi \rightarrow \pi^*$  [17], while the spectrum of  $\text{AuCl}_4^-$  solution showed a high intensity band at 212 nm and shoulder at 290 nm assigned to ligand to metal charge transfer transition (LMCT) [16,17]. The mixture of both reactants developed a pink color solution with strong absorption band appeared at 523 nm, Figure -1B assigned to the surface plasmon resonance (SPR) of spherical AuNPs [1-4, 20,21], with estimated size range about 10-23nm [22] indicating that  $\text{AuCl}_4^-$  has been reduced by ceftriaxone to form AuNPs. The proposed mechanism for the reduction process, illustrated in scheme-1 suggests that the  $\text{NH}_2$  group of thiazole ring, like any aromatic amine, may be responsible for the donation of electrons to  $\text{AuCl}_4^-$  according to the work published by C. Subramaniam on reduction of Au(III) ions by aromatic amines [23]. However the process was very slow that the solution had to be left for 24h to develop the color.

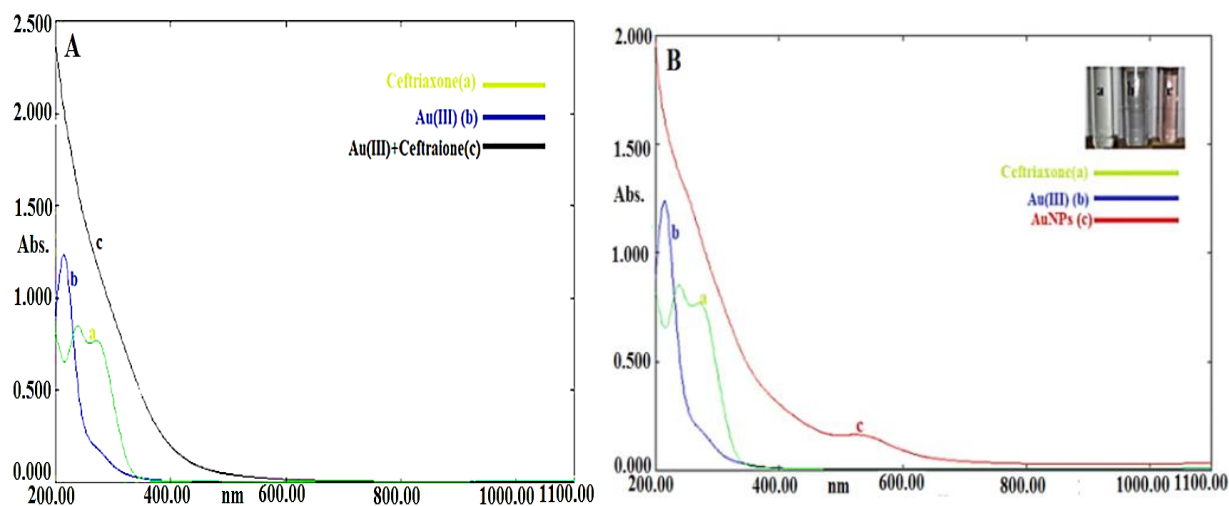
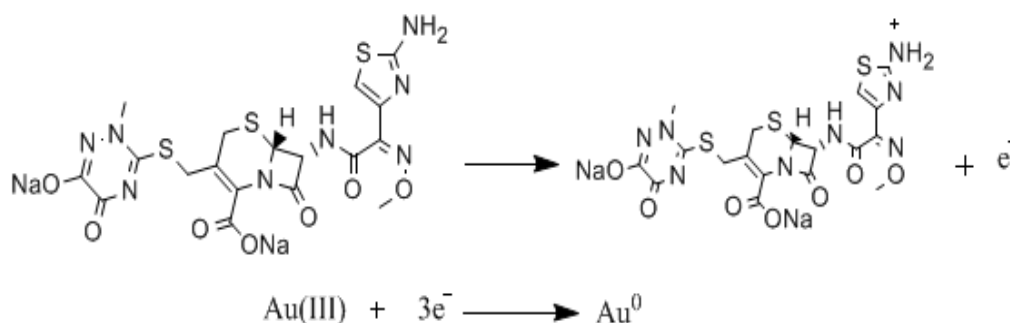


**Figure1-** The uv-visible spectra of a- Ceftriaxone, b-  $\text{AuCl}_4^-$  and c-synthesized gold nanoparticle in aqueous solutions at concentration ratio of CR/Au(III) (0.172), at room temperature A- after 1h and B- after 24h.



**Scheme 1-**Reduction of Au(III) ions with CR.

Figure-2 exhibits the variation of intensity and position of SPB of AuNPs solutions prepared from different concentration ratios of CR/Au(III) (2.41, 1.208, 0.805, 0.604, 0.48, 0.40, 0.302, 0.241, 0.201 and 0.172) respectively (1-10) and their performance after 1h, 24h, 48h, 1week, 2weeks and 3weeks (a-f respectively). No color change and no SPB were detected in all solutions at day of preparation. After 24h solutions of concentration ratio of CR/Au(III)(2.41-0.302) (solutions 1-7) showed no peaks of SPB of AuNPs and the solutions remained colorless, while the solutions of CR/Au(III)(0.241, 0.201 and 0.172) (8, 9 and 10 respectively), gave a peak at  $\lambda = 523, 535$  and  $523\text{nm}$  respectively corresponding to SPR of spherical AuNPs[1-4,20,21]. The three solutions remained stable for more than 3 weeks. The colors of solutions 5,6 and 7 were changed to pink and their spectra exhibited weak absorption bands at 540, 550 and 550 nm respectively after 48h with estimated size range 30-40nm[1,3] while no change was recorded by the solutions 1-4.

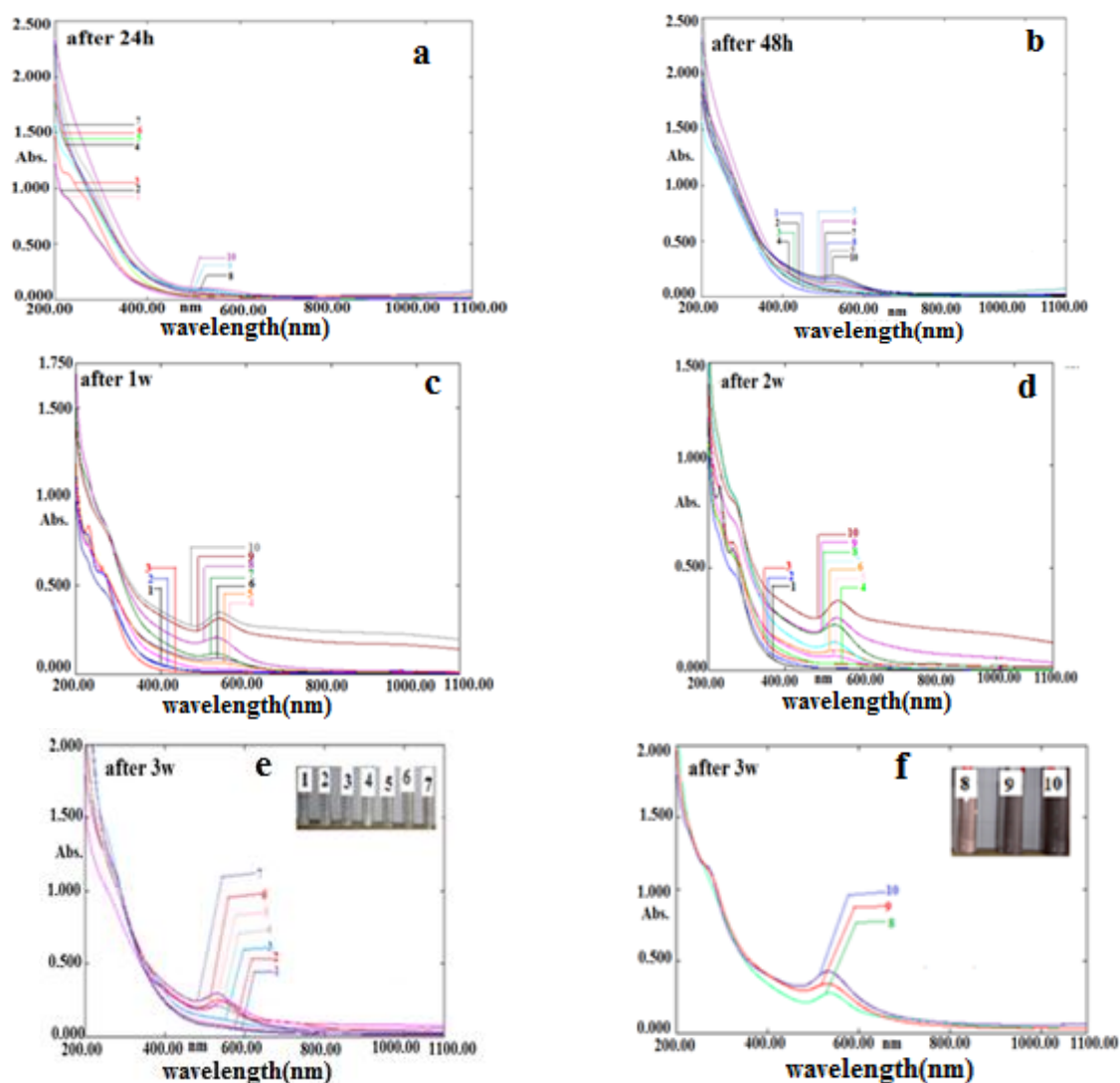


**Figure 2-** Absorption spectra with time of AuNPs prepared at different concentrations ratio of CR/Au(III) (2.41, 1.208, 0.805, 0.604, 0.48, 0.40, 0.302, 0.2416, 0.201 and 0.172) after 24h, 48h, 1week, 2week and 3week respectively(a- e, f).

These observations indicated that that CR is a weak reducing agent and its reducing capability increased with increased concentration of Au(III) ion. The synthesis of AuNPs by ceftriaxone best occurred at CR/Au (III) concentration ratios (0.241, 0.201 and 0.172 solutions 8-10 respectively). The reducing process may be more enhanced by seeding effect using some reducing agents prior to the addition of CR [24]. For higher rate of AuNPs, higher stability and smaller particle size. The synthesis of AuNPs was selected at concentration ratio of CR/Au(III) 0.172 which will be used for the study of pH and temperature effect on AuNPs.

### Effect of temperature on AuNPs synthesis

The synthesis of AuNPs were carried out at different temperatures using 10 aqueous solutions of CR and  $\text{AuCl}_4^-$  with concentration ratio of CR/Au(III) (0.172), which were heated at 35-80°C followed by cooling naturally to room temperature for 1h. The variations of spectra of these solutions with temperature are shown in Figure-3.

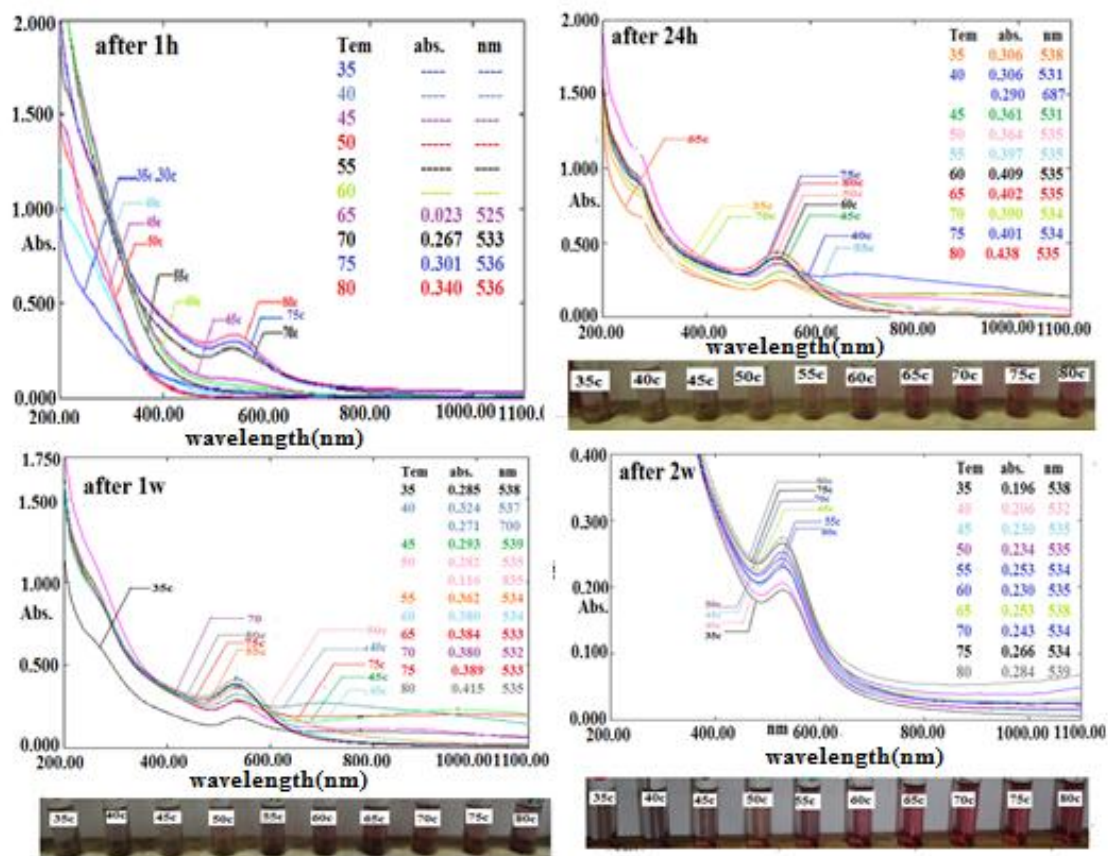
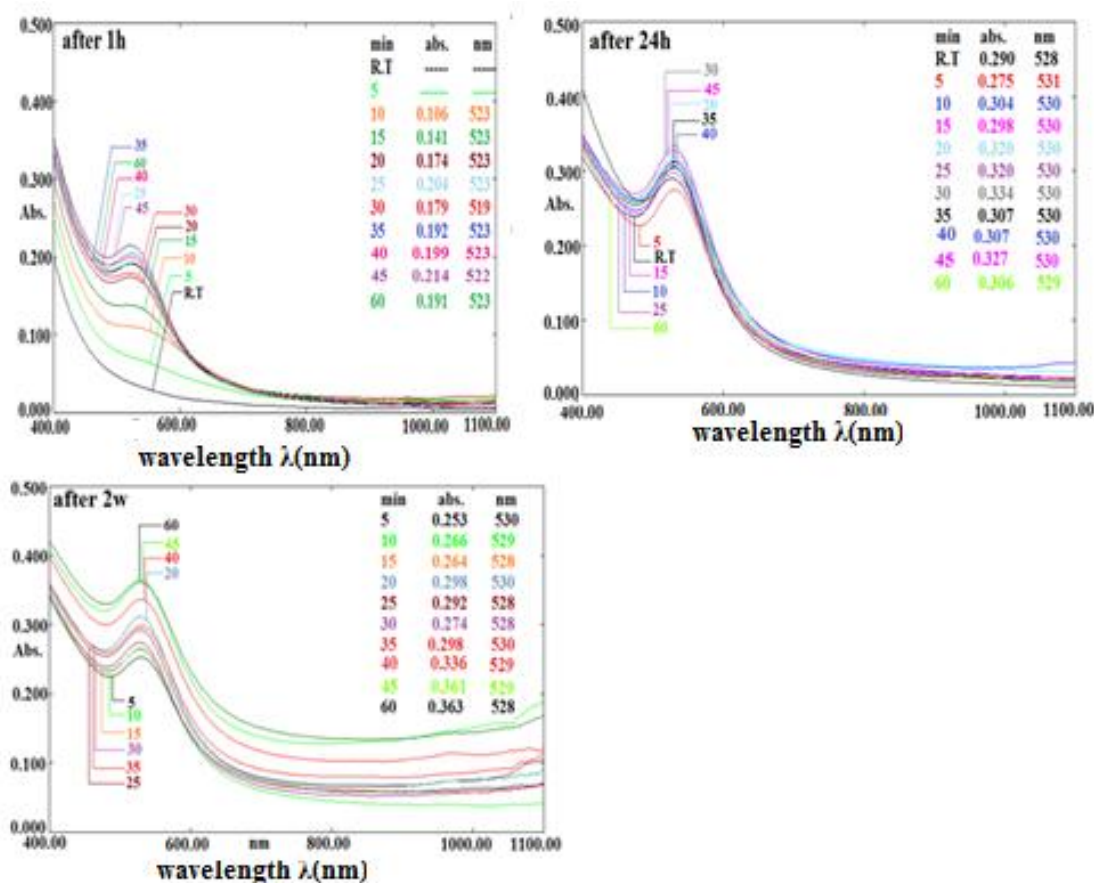


Figure 3-Absorption spectra with time of AuNPs aqueous solutions prepared from concentration ratio of CR/Au(III) =0.172 heated 35°C -80°C.

Color changes and SPB were observed only in the last four solutions at temperatures 65-80°C. The spectra of these solutions exhibited increased intensity with temperature of SPB of spherical AuNPs [1-4, 20, 21], which appeared at wavelength range (525, 533, 536 and 536 nm respectively). The other solutions had to be left for 24h to develop the color. Increasing the heating time from 5-10min at 40°C was found to exhibit pink color and the spectrum of the solution exhibited a single absorbance band at  $\lambda$ 523nm related to spherical AuNPs [1-4, 20, 21]. The solution was stable for two weeks with increased absorbance of SPB which was kept at wavelength range 529-530nm. The solution exhibited immediately color change when heating time was increased from 10-60 min and the absorption spectra of the colloid showed a single peak at wavelength range 523-532 nm referring to spherical AuNPs [1-4, 20,21] of size range 10-23nm [22]. The intensity of SPB was found to increase with time as is shown in Figure-4. The colloid was stable at room temperature for more than two weeks at the same wavelength range. The best heating time to give good particle size and stable AuNPs at 40°C for 45min.





**Figure 4-** Absorption spectra with time of AuNPs prepared from a solution of CR/Au(III) (0.172) heated at 40°C for different time periods (5-60min).

### Effect of pH

Figure-5 shows the absorption spectra of CR conjugated AuNPs prepared at CR/Au(III) concentration ratio (0.172) at different pH media (2.44, 3.38, 4.26, 5.83, 6.33, 7.20, 8.27, 9.03, 10.30 and 11.18) using the appropriate buffer. None of the studied solutions exhibited SPB of AuNPs at the same day of preparation. After 24h the first 5 solutions of pH values (2.44-6.33) (solutions 1-5) gave pink colors and the spectra of solutions 1, 2, 4 and 5 exhibited a single absorption band at  $\lambda$  563, 551, 530 and 526 nm respectively, related to spherical AuNPs [1-4, 20, 21], while the solution of pH=4.26 (solution 3) exhibited two high absorption bands at  $\lambda$  534 and 623 nm which may be attributed to the formation of nonspherical AuNPs [25-28]. After one week the spectrum of this solution showed only one band which appeared at  $\lambda$  551 nm.

The colors of solutions at pH 7.2, 9.03, 10.3 and 11.18 (solutions 6, 8-10 respectively) appeared only after two weeks and their spectra showed SPBs at  $\lambda$  538, 550, 542 and 539 nm respectively, while no color change was observed at pH 8.27 (solution 7). The highest rate of AuNPs synthesis was observed at pH 5.83 as the solution remained stable at the studied period without change in the position of SPB at  $\lambda$  533 nm. These results show that the difference in pH values plays an important role in controlling the synthesis, size and morphology of AuNPs which agrees with other studies mentioned in the literature [29, 30].

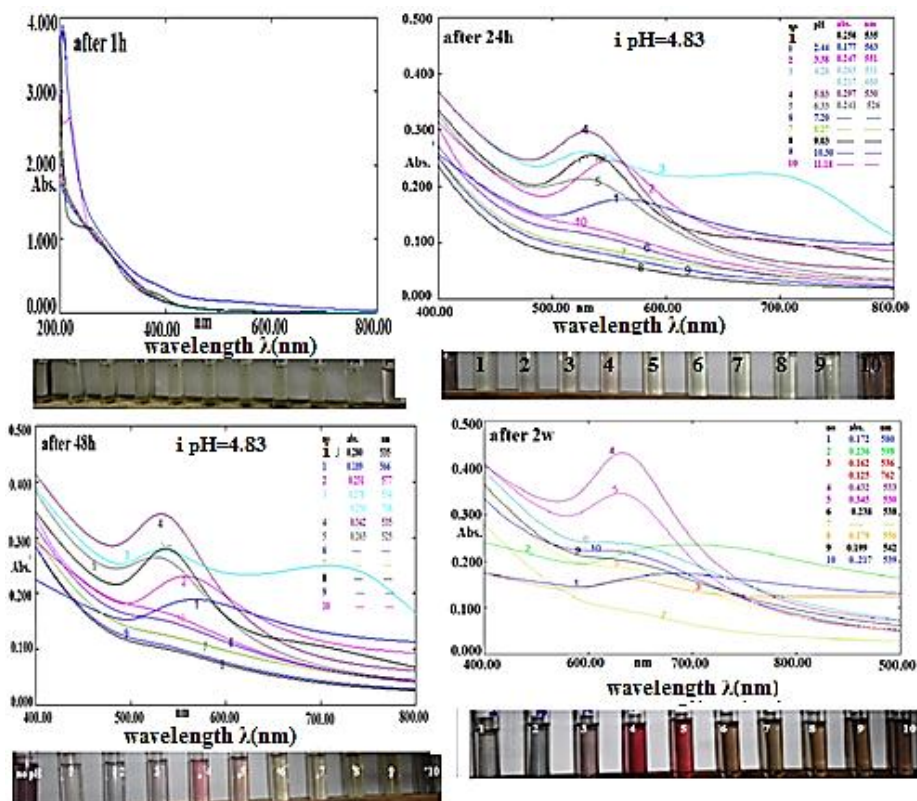


Figure 5-Absorption spectra with time of AuNPs prepared from a solution of CR/Au(III) (0.172) at different pH, i: initial pH.

2. FT-IR Spectra

The infrared spectrum of ceftriaxone, Figure -6a exhibited a band at 3444.63  $\text{cm}^{-1}$  attributed to the stretching vibration of free  $\text{NH}_2$  [14,31-33], while the band appeared at 3564.21  $\text{cm}^{-1}$  was due to  $\nu$  OH of  $\text{H}_2\text{O}$ [14]. The bands appeared at 3284.55, 1747.39 and 1649.02  $\text{cm}^{-1}$  were attributed N-H amide

[14],  $\nu(\text{C}=\text{O})$  b-lactam [31-33] and  $\nu(\text{C}=\text{O})$  amide [14,31-33] respectively. The absorption bands appeared at 1606.59 and 1415.65  $\text{cm}^{-1}$  are attributed to  $\nu_{\text{asy}}(\text{COO}^-)$  and  $\nu_{\text{sy}}(\text{COO}^-)$  vibrations respectively[31,32]. The peaks observed at 1539.09 and 1504.37  $\text{cm}^{-1}$  were associated with aromatic ring, The band at 1398.30  $\text{cm}^{-1}$  is due to  $\nu$  C-N[14,33]. The FT-IR spectrum of ceftriaxone-capped AuNPs is shown in Figure-6b.

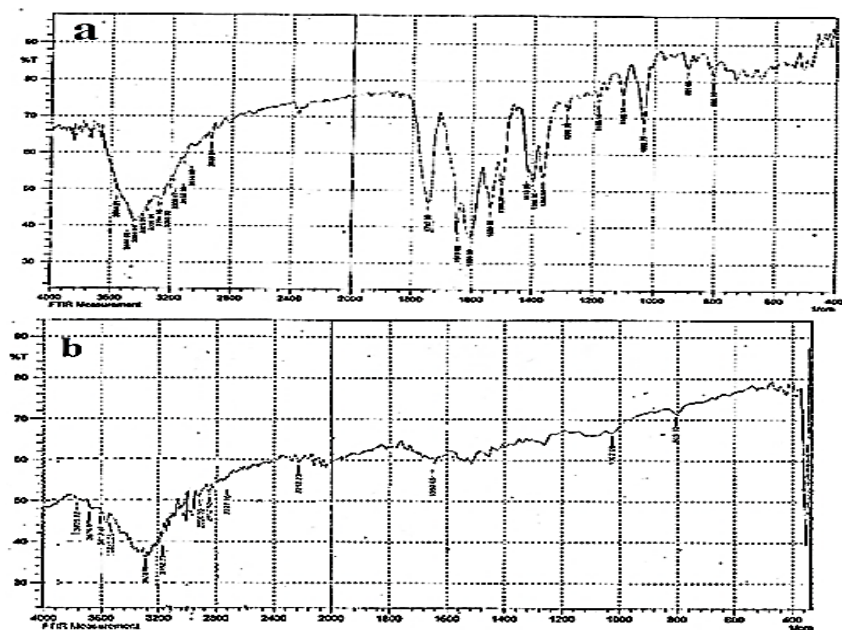


Figure 6-FT-IR spectra of a- ceftriaxone sodium and b- ceftriaxone-capped AuNPs.



The bands attributed to the stretching vibration of free  $\text{NH}_2$  was shifted to lower wavenumber and appeared at  $3251.76\text{cm}^{-1}$ . The bands assigned to  $\text{NH}$  amide and  $\nu \text{C}=\text{O}$  vibration of  $\beta$ -lactam were shifted to lower wavenumbers and appeared at  $3120.33\text{cm}^{-1}$  and  $1775\text{cm}^{-1}$  respectively while the bands attributed to amide  $\nu \text{C}=\text{O}$ ,  $\nu_{\text{asy}}(\text{COO}^-)$  and  $\nu_{\text{sy}}(\text{COO}^-)$  vibrations were shifted to higher wavenumbers and appeared at  $1675$ ,  $1650.95$  and  $1430.87\text{cm}^{-1}$  respectively. The band attributed to  $\nu \text{C}-\text{N}$  vibration was shifted to lower wavenumber and appeared at  $1027.90\text{cm}^{-1}$ . These data indicate that the functional groups of CR were covalently adsorbed on the surface of AuNPs.

### 3. X-ray Diffraction

The XRD patterns of AuNPs synthesized by ceftriaxone are shown in Figure-7. Four diffraction peaks were observed at  $2\theta = (38.3970, 44.5941, 64.7861 \text{ and } 77.7420)$  corresponding to the planes (111), (200), (220) and (311) respectively, the data of Bragg's reflection resembles the cubic structures of AuNPs, and refer to face centered cubic (fcc) Au metal crystal lattice[1,5]. The crystalline size of the nanoparticle can also be determined using Scherrer's equation [34-36].

$$D = \frac{K\lambda}{\beta \cos\theta}$$

Where  $D$  average crystalline size (nm),  $K$  (0.9) dimensionless shape factor,  $\lambda$  X-ray wavelength ( $1.541\text{ \AA}$ ),  $\theta$  angle of diffraction or Bragg angle (in radius) and  $\beta$  angular / line broadening at full width at half maximum (FWHM) of the XRD peak at the diffraction angle  $\theta$ . The average size of AuNPs was  $24.391\text{ nm}$ .

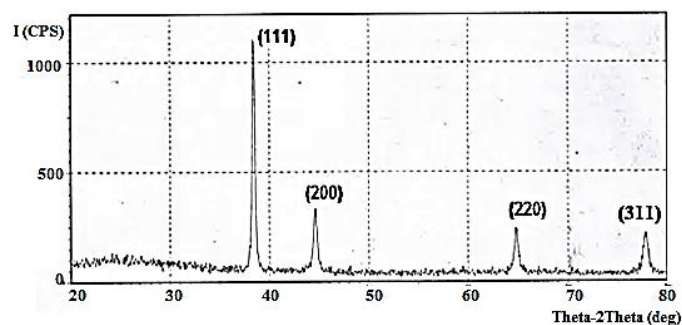


Figure 7-XRD pattern of ceftriaxone-capped AuNPs prepared at CR/Au(III) (0.172).

### 4. Scanning electron microscope (SEM) analysis

Figures-8 and -9 show the SEM images of AuNPs prepared from concentration ratio of CR/Au(III)= (0.172) and (0.241) respectively at room temperature. The particles in the first ratio Figures-8 appeared as large aggregates of different shapes between spherical to cubic, while the particles of the second ratio Figure-9 had more regular spherical shapes. The average diameters for both solutions were nearly the same ( $73.3$  and  $74.8\text{nm}$  respectively). Figure-10 shows the SEM micrograph of AuNPs prepared from a solution of concentration ratio CR/Au(III)=  $0.172$  after being heated at  $40^\circ\text{C}$  for  $45\text{ min}$ . The particles appeared nearly spherical in shape with the average diameter  $56.65\text{nm}$ .

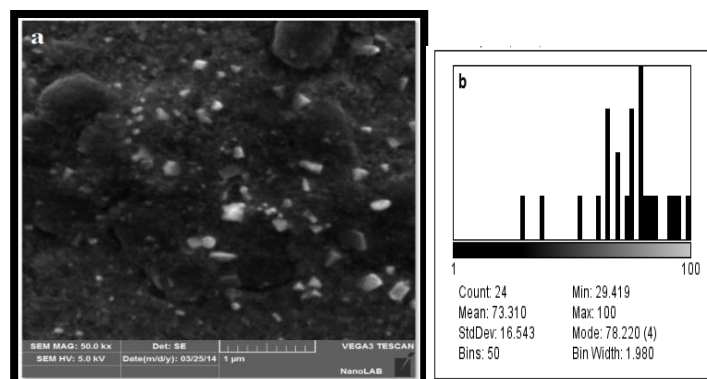


Figure 8-a-SEM and b-particle size distribution of ceftriaxone-synthesized AuNPs prepared from the concentration ratio CR/Au(III) 0.172 at room temperature.

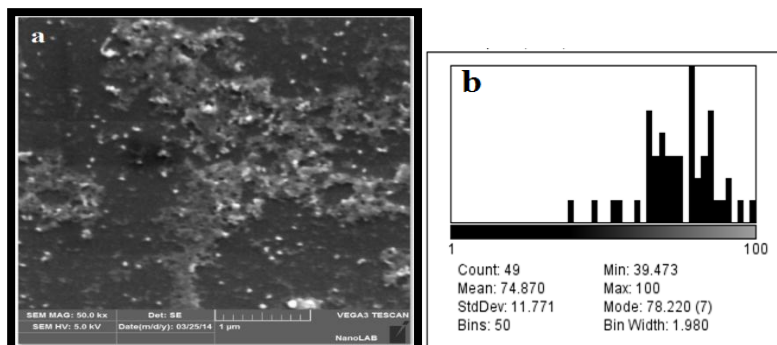


Figure 9-a-SEM and b-particle size distribution of ceftriaxone-synthesized AuNPs prepared from the concentration ratio CR/Au(III) 0.241 at room temperature.

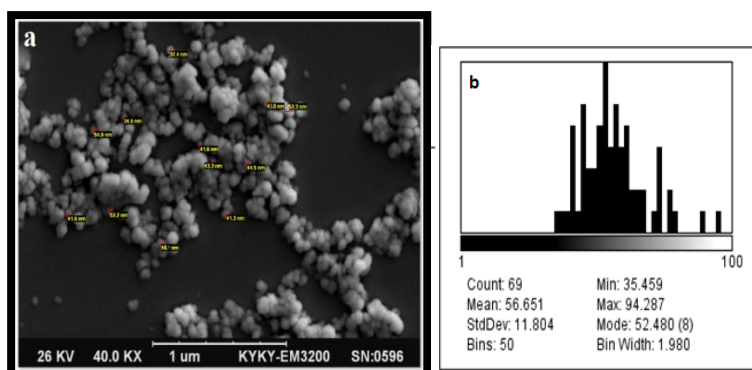


Figure 10-a-SEM and b-particle size distribution of ceftriaxone-synthesized AuNPs(CR-AuNPs)(CR/Au(III) =0.172) heated at 40°C for 45 min.

5. Atomic force microscope (AFM) analysis

Figures-11 and -12 and show the AFM of two and three dimensions images of CR-AuNPs prepared at room temperature from concentration ratio of CR/Au(III) =0.172 and 0.241 respectively which indicate the presence of spherical shapes of AuNPs. In contrast to the SEM analysis, there was a big difference in sizes between the two solutions as the particles obtained from CR/Au(III) = 0.241, Figure-12 showed larger sizes and a wider size distribution compared with that of CR/Au(III) = 0.172, Figure-11 which may be attributed to agglomerate nucleation during solution preparation. The average particle sizes were 59.50 and 111.05 nm respectively.

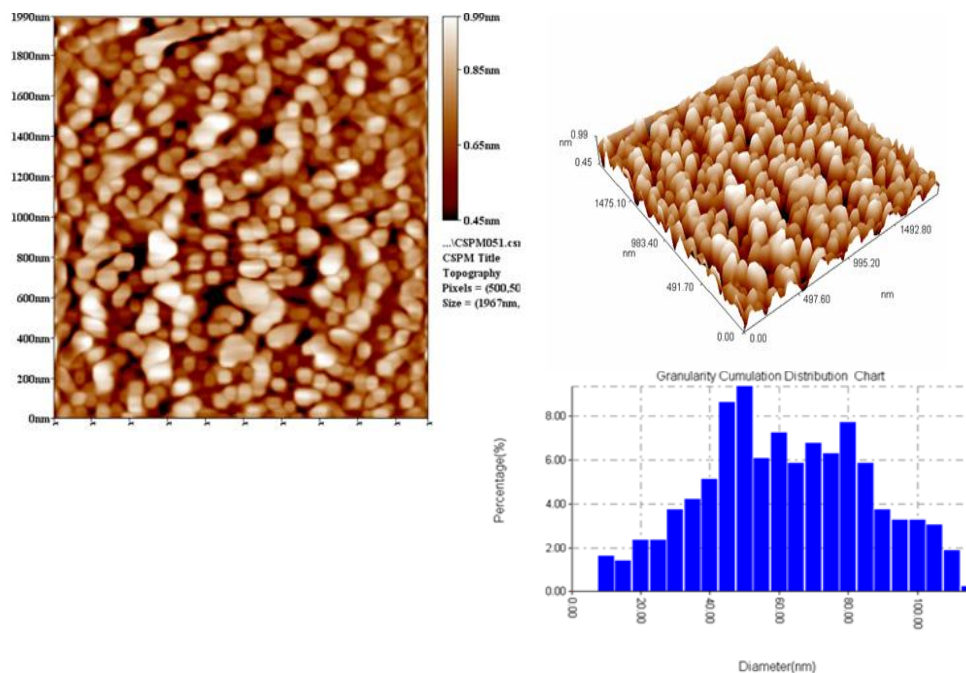
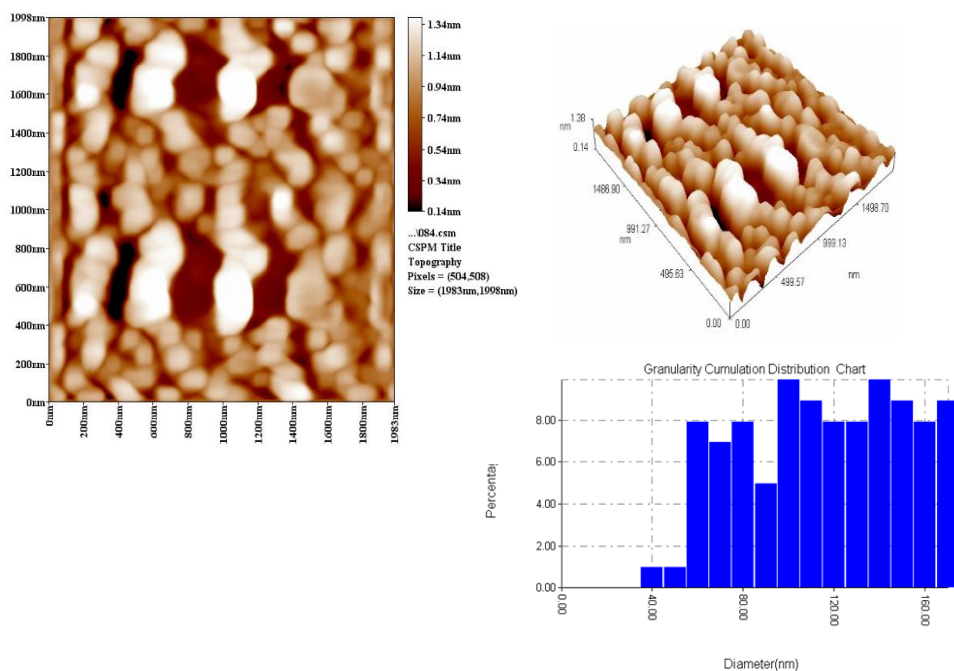
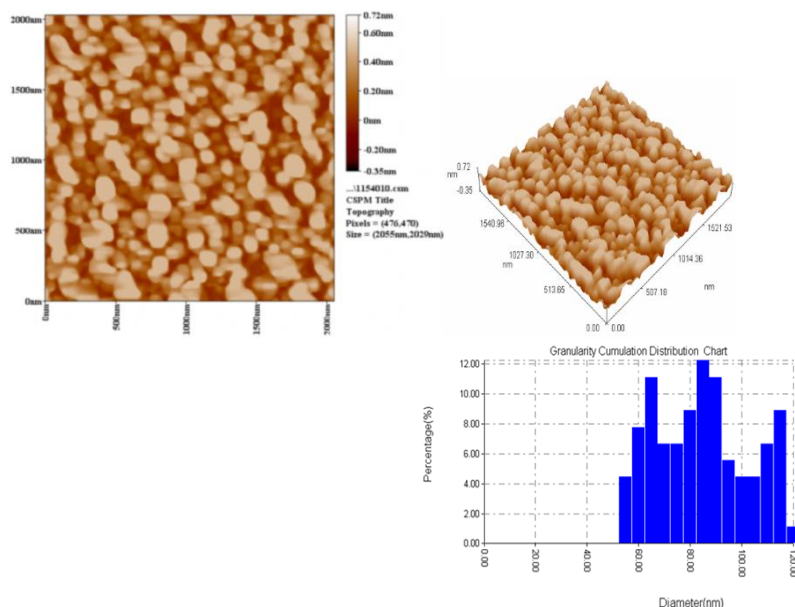


Figure 11-AFM 2D and 3D pictures and particle size distribution chart of the CR- AuNPs (CR/Au(III) 0.172) at room temperature( average diameter 59.50nm).



**Figure 12**-AFM 2D and 3D pictures and particle size distribution chart of CR- AuNPs at (CR/Au(III) 0.241) at room temperature, (average diameter around 111.05nm).

Figure-13 shows the AFM images of AuNPs prepared from concentration ratio of CR/Au(III)=0.172, heated at 40°C for 45 min, in which the particles were of spherical shapes with average diameter 82.23 nm. The results obtained from the SEM and AFM analysis in this work confirmed that reactant concentrations and temperature affected the sizes and morphology of AuNPs.



**Figure 13**-AFM 2D and 3D images and particle size distribution chart of the CR- AuNPs (CR/Au(III) (0.172) heated at 40 °C for 45 min ( average diameter 82.23nm).

### Antibacterial activity

The antibacterial activity of CR and its Au nanoparticle conjugated have been tested against four cultures of pathogenic bacteria namely: (*Escherichia coli*, *Pseudomonas aeruginosa*, *Staphylococcus aureus* and *Streptococcus pneumonia*) following the method reported by L. Baccigalupiet al[37], using drop diffusion method.

The results described in Table-1 show that the original antibiotic (CR) exhibited a high activity (17.5 mm) against *E. coli* only and was inactive against the other three cultures. This activity against *E. coli* was enhanced in the presence AuNPs and the diameter inhibition zone increased to 20 mm.

**Table 1-** Inhibition zone exhibited by CR its conjugated AuNPs against some pathogenic bacteria.

Type of ligand	Inhibition zone (mm)			
	<i>Escherichia Coli</i>	<i>Pseudomonas Aeruginosa</i>	<i>Staphylococcus aureus</i>	<i>Streptococcus Pneumonia</i>
CR	17.5	-	1	-
CR-capped AuNPs	20	-	1	1

### Conclusions

The synthesis as well as stability of AuNP conjugated with antibiotics ceftriaxone have been evaluated in absence of reducing agent at different reaction conditions of concentrations, pH and heating temperature ranges. The structure of sizes, morphology and stability of the synthesized AuNPs were highly dependent on reactant concentrations, temperature, heating time and pH as was indicated by uv-visible spectrophotometry. The synthesis of AuNPs were enhanced in moderately acidic medium and inhibited in basic medium. Sizes, morphology and crystallinity of the synthesized AuNPs were characterized by SEM, AFM and XRD respectively, while the conjugation with ceftriaxone was detected by FTIR spectrophotometry. Antibacterial activity screening of the antibiotic and its AuNPs conjugates showed that they were active against *Escherichia coli*, and inactive against *streptococcus*, *pseudomonas* and *staphylococcus aureus*. Ceftriaxone capped AuNPs exhibited higher antimicrobial activity against (*E. coli*) compared to ceftriaxone alone.

### Reference

1. Rai, A. Prabhune, A. and Perry, C.C. **2010**. Antibiotic mediated synthesis of gold nanoparticles with potent antimicrobial activity and their application in antimicrobial coatings. *Journal of Materials Chemistry*, 20, pp: 6789–6798.
2. Demurtas, M. and Perry, C.C. **2014**. Facile one-pot synthesis of amoxicillin-coated gold nanoparticles and their antimicrobial activity. *Gold Bull*, 47, pp: 103–107.
3. Brown, A. Smith, K. Samuels, T.A. Lu, J. Obare, S. and Scott, M.E. **2012**. Nanoparticles functionalized with ampicillin destroy multiple antibiotic resistant isolates of *Pseudomonas aeruginosa*, *Enterobacter aerogenes* and methicillin resistant *Staphylococcus aureus*. *Applied and Environmental Microbiology*, 78(8), pp:2768 –2774.
4. Bhattacharya, D. Saha, B. Mukherjee, A. Santra, C.R. and Karmakar, P. **2012**. Gold nanoparticles conjugated antibiotics: stability and functional evaluation. *Nanoscience and Nanotechnology*, 2(2), pp:14-21.
5. Zhang, Y. Wei, S. and Chen, S. **2013**. A facile and novel synthetic route to gold nanoparticles using cefazolin as a template for a sensor. *International Journal of Electrochemical Science*, 8, pp:6493 – 6501.
6. Hussain, R.K. **2014**. Synthesis and characterization of some new Schiff base derivatives of cefotaxime with their metal complexes and study the reduction of Au(III) ions to gold nanoparticles. M.Sc. Thesis. Department of Chemistry, College of Science, University of Baghdad. Baghdad, Iraq.
7. Hameed, A. Islam, N. Shah, M.R. and Kanwal, S. **2011**. Facile one-pot synthesis of gold nanoclusters and their sensing protocol. *Chemical Communication Journal*, 47, pp:11987-11989.
8. Maradiya, J.J. Goriya, H.V. Bhavsar, S.K. Maradiya, J.J. Goriya, H.V. Bhavsar, S.K. Patel, U.D. and Thaker, A.M. **2010**. Pharmacokinetics of ceftriaxone in calves. *Veterinarski Arhiv*, 80(1), pp:1-9.
9. Durairaj, S. Annadurai T. Kumar, B.P. and Arunkumar, S. **2010**. Simultaneous estimation of ceftriaxone sodium and sulbactamsodium using multi-component mode of analysis. *International Journal of ChemTechResearch*, 2(4), pp:2177-2181.

10. Gurupadaya, B. M. and Disha, N.S. **2013**. Stability indicating HPLC method for the simultaneous determination of ceftriaxone and vancomycin in pharmaceutical formulation. *Journal of Chromatography and Separation Techniques*, 4(10), pp:1-5.
11. Shah, J. Jan, M.R. Shah, S. and Khan, M.N. **2013**. Development and validation of HPLC method for simultaneous determination of ceftriaxone and cefaclor in commercial formulations and biological samples. *Journal of the Mexican Chemical Society*, 57(4), pp:314-320.
12. Kumar, R.N. Rao, G.N. and Naidu, P.Y. **2012**. Stability indicating fast LC method for determination of ceftriaxone and tazobactam for injection related substances in bulk and pharmaceutical formulation. *International Journal of Applied Biology and Pharmaceutical Technology*, 1(1), pp:145-157.
13. Sabale, P.M. Kaur, P. Patel, Y. Patel, J. and Patel, R. **2012**. Metalloantibiotics in therapy: an overview. *Journal of Chemical and Pharmaceutical Research*, 4(11), pp:4921-4936.
14. Song, Y. Zhu, A. Song, Y. Cheng, Z. Xu, J. and Zhou, J. **2012**. Experimental and theoretical study on the synthesis of gold nanoparticles using ceftriaxone as a stabilizing reagent for and its catalysis for dopamine. *Gold Bull*, 45, pp:153-160.
15. Aslam, M. Fu, L. Su, M. Vijayamohan, K. and Dravid, V.P. **2004**. Novel one-step synthesis of amine-stabilized aqueous colloidal gold nanoparticles. *Journal of Materials Chemistry*, 14, pp:1795-1797.
16. Sun, X. Dong, S. and Wang, E. **2006**. One-step polyelectrolyte-based route to well-dispersed gold nanoparticles: synthesis and insight. *Materials Chemistry and Physics*, 96, pp:29-33.
17. Pasha, C. and Narayana, B. **2008**. A simple method for the spectrophotometric determination of cephalosporins in pharmaceuticals using variamine blue. *Eclética Química*, 33(2), pp:41-46.
18. Link, S. and El-Sayed, M.A. **1999**. Size and temperature dependence of the plasmon absorption of colloidal gold nanoparticles. *Journal of Physical Chemistry*, 103, pp:4212-4217.
19. Jiang, G. Wang, L. and Chenv, W. **2007**. Studies on the preparation and characterization of gold nanoparticles protected by dendrons. *Materials Letters*, 61(1), pp:278-283.
20. Zhang, L. Swift, J. Butts, C.A. Yerubandi, V. and Dmochowski, I.J. **2007**. Structure and activity of apoferritin-stabilized gold nanoparticles. *Journal of Inorganic Biochemistry*, 101, pp:1719-1729.
21. Manson, J. Kumar, D. Meenan, B.J. and Dixon, D. **2011**. Polyethylene glycol functionalized gold nanoparticles: the influence of capping density on stability in various media. *Gold Bull*, 44(2), pp:99-105.
22. Jayalakshmi, K. Ibrahim, M. and Rao, K.V. **2014**. Effect of pH on the size of gold nanoparticles. *International Journal of Electronic and Electrical Engineering*, 7(2), pp:159-164.
23. Subramaniam, C. Tom, R.T. and Pradeep, T. **2005**. On the formation of protected gold nanoparticles from  $\text{AuCl}_4^-$  by the reduction using aromatic amines. *Journal of Nanoparticle Research*, 7, pp:209-217.
24. Sau, T.K. Pal, A. Jana, N.R. Wang, Z.L. and Pal, T. **2001**. Size controlled synthesis of gold nanoparticles using photochemically prepared seed particles. *Journal of Nanoparticle Research*, 3, pp:257-261.
25. Boopathi, S. Senthilkumar, S. and Phani, K.L. **2012**. Facile and one pot synthesis of gold nanoparticles using tetraphenylborate and polyvinyl pyrrolidone for selective colorimetric detection of mercury ions in aqueous medium. *Journal of Analytical Methods in Chemistry*, 2012, pp:1-6.
26. Johan, M.R. Chong, L.C. and Hamizi, N.A. **2012**. Preparation and stabilization of monodisperse colloidal gold by reduction with monosodium glutamate and poly(methylmethacrylate). *International Journal of Electrochemical Science*, 7, pp:4567-4573.
27. Shi, W. Casas, J. Venkataramasubramani, M. and Tang, L. **2012**. Synthesis and characterization of gold nanoparticles with plasmon absorbance wavelength tunable from visible to near infrared region. *International Scholarly Research Network ISRN Nanomaterials*, 2012, pp:1-9.
28. Samal, A.K. Sreepasad, T.S. and Pradeep, T. **2010**. Investigation of the role of  $\text{NaBH}_4$  in the chemical synthesis of gold nanorods. *Journal Nanoparticle Research*, 12, pp:1777-1786.
29. Shan, C. Li, F. Yuan, F. Yang, G. Niu, L. and Zhang, Q. **2008**. Size-controlled synthesis of monodispersed gold nanoparticles stabilized by polyelectrolyte-functionalized ionic liquid. *Nanotechnology*, 19, pp:1-6.



30. Li, C. Li, D. Wan, G. Xu, J. and Hou, W. **2011**. Facile synthesis of concentrated gold nanoparticles with low size-distribution in water: temperature and pH controls. *Nanoscale Research Letters*, 6(440), pp:1-10.
31. Anacona, J.R. and Lopez, M. **2012**. Mixed-ligand nickel(II) complexes containing sulfathiazole and cephalosporin antibiotics: synthesis, characterization, and antibacterial activity. *International Journal of Inorganic Chemistry*, 2012, pp:1-8.
32. Reiss, A. Chifiriuc, M.C. Amzoiu, E. and Spînu C.I. **2014**. Transition metal(II) complexes with cefotaxime-derived Schiff base: synthesis, characterization, and antimicrobial studies. *Bioinorganic Chemistry and Applications*, 2014, pp:1- 17.
33. El-Said, A.I. Aly, A.A.M. El-Meligy, M.S. and Ibrahim, M.A. **2009**. Mixed ligand Zinc(II) and Cadmium(II) complexes containing ceftriaxone or cephradine antibiotics and different donors. *The Journal of the Argentine Chemical Society*, 97(2), pp:149-165.
34. Firdhouse, M.J. Lalitha, P. and Sripathi, S.K. **2014**. An undemanding method of synthesis of gold nanoparticles using *Pisoniagrandsis* (R. Br.). *Digest Journal of Nanomaterials and Biostructures*, 9(1), pp:385 – 393.
35. Kaidanovych, Z. Kalishyn, Y. and Strizhak, P. **2013**. Deposition of monodisperse platinum nanoparticles of controlled size on different Supports. *Advances in Nanoparticles*, 2, pp:32-38.
36. Monshi, A. Foroughi, M.R. and Monshi, M.R. **2012**. Modified Scherrer equation to estimate more accurately nano-crystallite size using XRD. *World Journal of Nano Science and Engineering*, 2, pp:154-160.
37. Baccigalupi, L. Donato, A. Parlato, M. Luongo, D. Carbone, V. and Rossi, M. **2005**. Two small, surface-associated factors mediate adhesion of a food-isolated strain of *Lactobacillus fermentum* to caco cell. *Research Microbial*, 156, pp:830-836.